

Effect of thermomechanical processing on grain boundary character distribution of a Ni-based superalloy

L. Tan *, K. Sridharan, T.R. Allen

Department of Engineering Physics, University of Wisconsin-Madison, 1500 Engineering Drive, Madison, WI 53706, USA

Abstract

Grain boundary engineering (GBE) was performed on an INCONEL alloy 617 by means of thermomechanical processing (TMP) to optimize the grain boundary character distribution (GBCD) with an increased fraction of low- Σ coincidence site lattice boundaries (CSLBs). Samples with a 5% thickness reduction followed by annealing at 1100 °C for 90 min promoted more low- Σ CSLBs than those with greater thickness reductions. The fraction of the $\Sigma 3''$ ($\Sigma 3$, $\Sigma 9$, and $\Sigma 27$) boundaries was promoted preferentially by TMP, which is desirable for the improvement of material's properties. The thermal stability of the GBE-optimized GBCD was verified to be stable at 850 °C for 672 h without significant degradation.

© 2007 Elsevier B.V. All rights reserved.

1. Introduction

The Ni-based superalloy, INCONEL 617 (UNS N06617), has been broadly utilized in gas turbines for combustion cans and ducts as well as industrial furnace components and applications where high-temperature corrosion resistance is generally important. Based on its excellent resistance to oxidation in a wide range of corrosive media and excellent high temperature strength, alloy 617 had been selected as a potential candidate alloy for Generation IV nuclear plant designs [1]. Alloy 617 is an austenitic solid-solution alloy with a composition Ni–22Cr–13Co–10Mo (wt%). It is normally used in a solution-annealed condition which provides a coarse

grain structure for the best creep-rupture strength. However, to withstand the high temperature and pressure environments in modern and future power plant system, the properties of alloy 617 could benefit from further improvement for extending its service lifetime and thus maintaining system stability.

Grain boundary engineering (GBE), proposed by Watanabe [2] in the early 1980s, has been extensively investigated as an approach to improve properties such as creep [3] and stress corrosion cracking resistance [4], by promoting a high proportion of low- Σ ($\Sigma \leq 29$) coincidence site lattice boundaries (CSLBs) in materials. In the nomenclature of the CSL model, the newly formed superlattice is denoted by a value of Σ , where the Σ value is defined as the reciprocal of the fraction of lattice points in the boundaries that coincide between the two adjoining grains. Thus, there is a low distortion of atomic bonds and relatively small free volume for CSLBs and consequently result in low boundary

* Corresponding author. Tel.: +1 608 262 7476; fax: +1 608 263 7451.

E-mail address: lizhentan@wisc.edu (L. Tan).

energies. Detailed information about the CSL model and CSL effect on GBE may be found in Ref. [5].

Based on our previous work on GBE of INCOLOY alloy 800H, which demonstrated significant improvement on oxide stability by GBE during exposure to supercritical water [6], the GBE approach was investigated for alloy 617 with the goal of understanding the effect of thermomechanical processing on grain boundary character distribution (GBCD).

2. Experiment

Commercial alloy 617, which was solution annealed at a temperature of 1176 °C for a time commensurate with section size followed by water quenching, was procured from special metals for this study. Its chemical composition is shown in Table 1. Various combinations of cold rolling and annealing were employed as the thermomechanical processes to achieve GBE effects on the as-received samples. Based on previous experience with GBE of an austenitic alloy 800H [7], an annealing temperature, 1100 °C, followed by water quenching was used to ensure a single phase austenite. Three levels of thickness reduction (5%, 9%, and 13%), different annealing times (15, 30, 45, 60, and 90 min), and multiple cycles of thermomechanical processing were employed in this study to investigate their effect on GBCD.

Electron backscatter diffraction (EBSD) was employed for the determination of grain boundary misorientations using the TSL orientation imaging microscopy (OIM) system MSC2200 attached to a field-emission scanning electron microscope LEO 1530 FESEM. To obtain good quality EBSD patterns, the samples were mechanically polished with SiC abrasive paper down to 1200 grit followed by sequential polishing with 1 µm diamond paste, alpha alumina and colloidal silica solutions. The SEM was operated at 20 kV, and the automatic EBSD area scan was performed over an area of 500 × 1000 µm² using a hexagonal grid with a step size of 5 µm. The number of scanned grains was about 1100 for each of the samples, which provided statis-

tically significant results. To allow for the identification of phases with the EBSD analytical software, a crystallographic data file was established based on X-ray diffraction analysis. For phase analysis with EBSD, a voting scheme and the confidence index (CI) established by TSL were used [8]. A high number of votes and higher CI values indicate a higher possibility that the phase is correctly identified. The character of grain boundaries in all samples were classified according to the Brandon criterion [9] for the maximum allowable misorientation ($\Delta\theta$) from the exact CSL as given by: $\Delta\theta = \Delta\theta_m \Sigma^{-1/2}$, where θ_m is the maximum misorientation angle for a low-angle boundary (typically, 15°).

3. Results and discussion

As-received samples were subjected to a variety of thickness reductions and thermomechanical processing (TMP) cycles. The average grain size of as-received and GBE-treated samples is 22 µm and 25 µm, respectively. The minor enlargement of the grain size is reasonable because some random boundaries were transformed to coherent $\Sigma 3$ boundaries. Because coherent $\Sigma 3$ boundaries are immobile and not a constituent of the intergranular transport network, they were not counted as grain boundaries during grain size measurement by defining a 60° rotation about the $\langle 111 \rangle$ crystal direction with a 5° misorientation tolerance.

3.1. GBCD of as-received and GBE-treated samples

The EBSD analyzed GBCD of the GBE-treated samples, as well as as-received sample, are shown in Fig. 1. GBCD is composed of three categories of boundaries: $\Sigma 1$, low- Σ CSLBs ($3 \leq \Sigma \leq 29$), and random boundaries. $\Sigma 1$ boundaries may be introduced by deformation-induced texture, which increases the probability that grains having almost the same orientation will reside as neighbors. In addition, the presence of many sub-boundaries in the material [5] and the recombination of two like boundaries impinging on each other [10] will also increase the $\Sigma 1$ fraction. Thus, the fraction of low- Σ CSLBs does not include the contribution from

Table 1
Composition of the as-received INCONEL alloy 617 (wt%)

Ni	Cr	Co	Mo	Al	Fe	Ti	Si	Mn	C	Cu	S	B
>51.4	21.7	12.4	10.9	1.2	1.2	.3	.2	.05	~.1	<.05	<.015	<.006

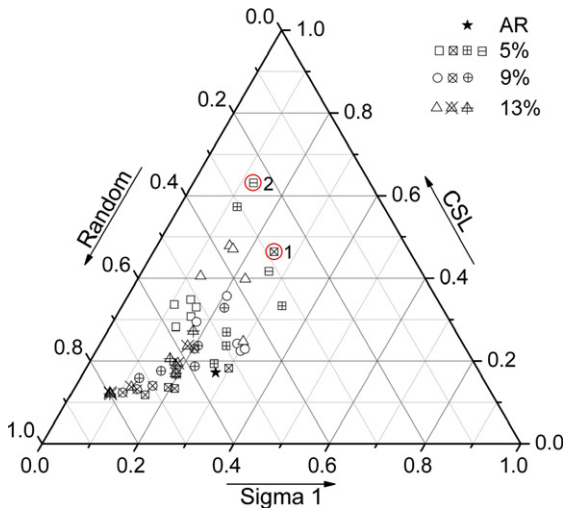


Fig. 1. Grain boundary character distribution (GBCD: $\Sigma 1$, low- Σ CSLBs ($\Sigma 3$ – $\Sigma 29$), and *random* boundaries) of the as-received (AR) and GBE-treated samples as a function of initial percentage reduction in thickness (5%, 9%, and 13%). The symbols in open, diagonal cross, cross, and single horizontal bar denote the number of thermomechanical cycles from 1 to 4 applied to the samples. The two data points highlighted with circle represent good GBE-treated conditions with similar low fraction of random boundaries, which are denoted as GBE1 and GBE2.

$\Sigma 1$ due to ambiguities in distinguishing these interfaces from sub-boundaries present in materials. Random boundaries are large-angle boundaries excluding the low- Σ CSLBs. Fig. 1 shows that a large thickness reduction did not significantly increase the low- Σ CSLBs fraction or even reduce the fraction of the low- Σ CSLBs. This may be because the internal energy introduced by cold work could not be easily released following annealing to promote the transformation from random boundaries to low- Σ CSLBs. In addition, the low- Σ CSLBs increased by the previous TMP cycle may be not able to be retained during the next TMP cycle with a high thickness reduction. Optimal GBE-treatment was achieved by multiple TMP cycles with 5% thickness reduction. Two representative conditions of the GBE-treated samples are highlighted with circles in Fig. 1 and denoted as GBE1 and GBE2. These two GBE-treated samples possess a similar low fraction of random boundaries ($\sim 27\%$). The major difference is that GBE2 has a $\sim 13\%$ smaller fraction of $\Sigma 1$ boundaries (or a higher fraction of low- Σ CSLBs) compared to GBE1.

The fraction of the low- Σ CSLBs components for the as-received and the two GBE-treated samples (GBE1 and GBE2) are shown in Fig. 2. It is clear

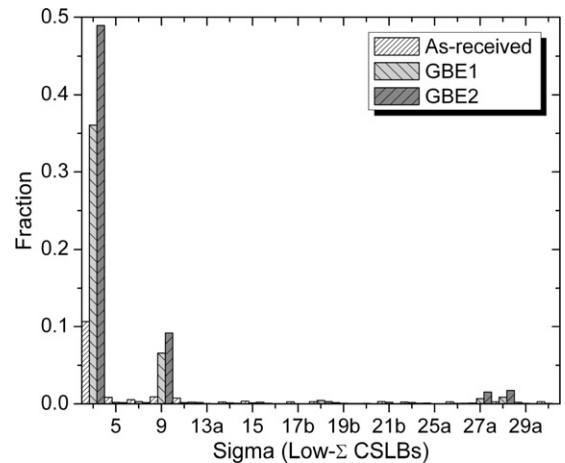


Fig. 2. Fraction of low- Σ CSLBs of the as-received and GBE-treated samples, GBE1 and GBE2.

that the fractions of $\Sigma 3^n$ ($\Sigma 3$, $\Sigma 9$, and $\Sigma 27$) boundaries were greatly enhanced for GBE-treated samples, GBE1 and GBE2. The fraction of $\Sigma 3$ boundaries of GBE1 and GBE2 increased to $\sim 36\%$ and $\sim 49\%$, respectively, compared to the $\sim 11\%$ for the as-received sample. The fractions of $\Sigma 9$ and $\Sigma 27$ boundaries of GBE1 and GBE2 were about 5–9 and 7–10 times of the as-received sample, respectively. The increased fractions of $\Sigma 3^n$ boundaries indicate that a lot of twinning and multiple twinning events occurred during annealing after cold rolling to $\sim 5\%$. This is desirable for property improvement of materials [3–5,11]. As shown in Fig. 2, the fraction of $\Sigma 3^n$ boundaries of GBE2 is $\sim 17\%$ higher than that of GBE1 in addition to the difference in the fraction of $\Sigma 1$ boundaries shown in Fig. 1.

The effect of the TMP on the fraction of low- Σ CSLBs can also be represented by the deviations from exact Σ misorientation [7,10]. The deviation from the exact $\Sigma 3$ misorientations of as-received and GBE-treated samples is shown in Fig. 3. The GBE2 sample, which has the highest fraction of $\Sigma 3$ boundaries, shows the smallest deviation from the exact $\Sigma 3$ compared to the as-received and GBE1 samples.

INCONEL alloy 617 is a face-centered-cubic alloy with moderate stacking fault energy (SFE). The low SFE promotes twin formation ($\Sigma 3$) during annealing after plastic deformation. The dependence of twin density (ρ , $\Sigma 3$) upon the SFE and grain size (d) of material could be described by a simple equation: $\rho = \frac{b}{d} \log \frac{d}{d_0}$ [12], where b is a

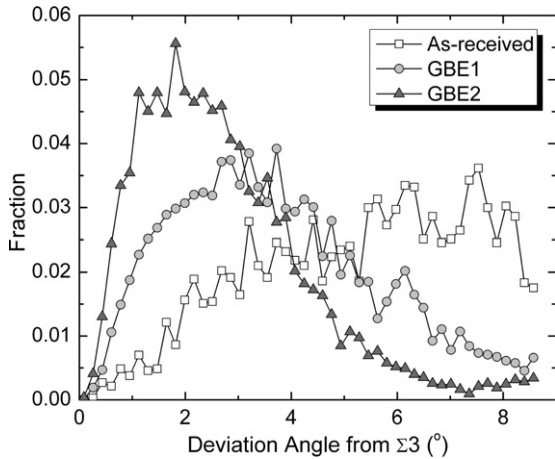


Fig. 3. Deviation angle from exact $\Sigma 3$ of the as-received and GBE-treated samples, GBE1 and GBE2.

constant related to the inverse of the SFE of the material, and d_0 is the grain size at which $\rho = 0$. Therefore, lower SFE and smaller grain size would produce a higher fraction of $\Sigma 3$ boundaries.

3.2. Thermal stability of GBE-optimized GBCD

Since atomic migration is promoted at elevated temperature, TMP-promoted low- Σ CSLBs may become unstable and be transformed into random boundaries. Thus, it is necessary to evaluate the thermal stability of GBE-optimized GBCD of samples. The fraction change of $\Sigma 1$, low- Σ CSLBs and random boundaries due to annealing at 850 °C for

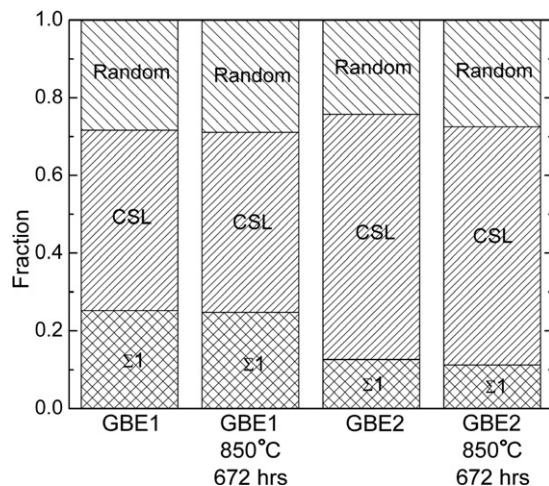


Fig. 4. Thermal stability of the grain boundary character distribution of GBE-treated samples, GBE1 and GBE2, after exposure at 850 °C for 672 h.

672 h is shown in Fig. 4. The selection of the annealing temperature, 850 °C, refers to the design of Generation IV nuclear reactor, e.g. the outlet temperature of the gas-cooled fast reactor (GFR) [13]. It is clear that the fraction change is insignificant for the GBE-treated samples (GBE1 and GBE2). In addition, the change of the fraction of $\Sigma 3^n$ boundaries is less than 1%. Longer annealing time at 850 °C is in progress. Even though alloy 617, because of its high cobalt concentration, is not applicable for in-core components, the processing developed for alloy 617 may be transferable to other Ni-base alloys.

4. Conclusion

INCONEL alloy 617 is a potential candidate alloy for application in future nuclear reactors. Grain boundary engineering (GBE) by means of thermomechanical processing (TMP) was investigated for this material because it is prone to twin formation due to its moderate stacking fault energy. Three levels of thickness reduction (5%, 9%, and 13%) followed by annealing for different time intervals were performed on the as-received material. The grain boundary character distribution (GBCD) of the as-received and GBE-treated samples was analyzed by electron backscatter diffraction (EBSD). The GBCD was optimized by a 5% thickness reduction followed by annealing at 1100 °C for 90 min, and more effectively with multiple TMP cycles. The fraction of the $\Sigma 3^n$ ($\Sigma 3$, $\Sigma 9$, and $\Sigma 27$) boundaries was promoted significantly by TMP, which is ~ 5 times of that of the as-received sample. The thermal stability of the GBE-optimized GBCD was confirmed at 850 °C for 672 h.

Acknowledgements

This material is based upon the work supported by the US Department of Energy under Award No. DE-FG07-03ID14542.

This report was prepared as an account of work sponsored by an agency of the United States Government. Neither the United States Government nor any agency thereof, nor any of their employees, makes any warranty, express or implied, or assumes any information, apparatus, product, or process disclosed, or represents that its use would not infringe privately owned rights. Reference herein to any specific commercial products, process, or service by trade name, trademark, manufacturer,

or otherwise does not necessarily constitute or imply its endorsement, recommendation, or favoring by the United States Government or any agency thereof. The views and opinions of authors expressed herein do not necessarily state or reflect those of the United States Government or any agency thereof.

References

- [1] Next generation nuclear plant materials research and development program plan, Idaho National Engineering and Environmental Laboratory, Bechtel BWXT Idaho, LLC, September 2004, INEEL/EXT-04-02347.
- [2] T. Watanabe, Res Mech. 11 (1984) 47.
- [3] D.S. Lee, H.S. Ryoo, S.K. Hwang, Mater. Sci. Eng. A 354 (2003) 106.
- [4] M. Shimada, H. Kokawa, Z.J. Wang, Y.S. Sato, I. Karibe, Acta Mater. 50 (2002) 2331.
- [5] V. Randle, The Role of the Coincidence Site Lattice in Grain Boundary Engineering, The Institute of Materials, London, 1996.
- [6] L. Tan, K. Sridharan, T.R. Allen, J. Nucl. Mater. 348 (2006) 263.
- [7] L. Tan, T.R. Allen, Mater. Met. Trans. A 36 (2005) 1921.
- [8] D.P. Field, Ultramicroscopy 67 (1997) 1.
- [9] D.G. Brandon, Acta Metall. 14 (1966) 1479.
- [10] A.J. Schwartz, W.E. King, JOM 50 (1998) 50.
- [11] V.Y. Gertsman, S.M. Bruemmer, Acta Mater. 49 (2001) 1589.
- [12] B.B. Rath, M.A. Imam, C.S. Pande, Mater. Phys. Mech. 1 (2000) 61.
- [13] A Technology Roadmap for Generation IV Nuclear Energy Systems, Issued by the US DOE Nuclear Energy Research Advisory Committee and the Generation IV International Forum, December 2002. (<<http://gif.inel.gov/roadmap/>>).